MRS Advances

Data-driven Sliding Mode Control for Pulses of Fluorescence in STED Microscopy Based on Förster Resonance Energy Transfer Pairs

Maison Clouatre and Makhin Thitsa

Department of Electrical and Computer Engineering, Mercer University, Mercer University Drive, Macon, GA 31207, USA

ABSTRACT

Pairs of conjugate donor-acceptor fluorescent probes have proven themselves useful in stimulated emission depletion (STED) microscopy in recent years. For instance, it has been shown that the lifetime of said probes directly correlates to the resolution of the microscope. However, once the lifetimes of the probes have been optimized, it is desirable to control their fluorescence in order to improve the resolution further. Here, we propose combining model-free control with sliding mode control to track nanosecond pulses of red-shifted acceptor fluorescence in order to inhibit visible light emitted from the image plane, shrink the point spread function, and subsequently improve the resolution of the microscope. This is achieved by automatic adjustment of the STED laser beam pump power. This controller is numerically simulated against a generic model created from Förster resonance energy transfer (FRET) theory. However, since it is data-driven, it can be easily applied to various physical systems with drastically different dynamics. This work provides a reliable theoretic control solution to modern super resolution microscopy for biological imaging.

INTRODUCTION

Stimulated emission depletion (STED) microscopy has gained attention in recent years in the field of biological imaging and earned the 2014 Nobel Prize in Chemistry. Using a unique array of laser beams, the STED microscope images beyond Abbe's diffraction limit of light [1-5]. While an excitation laser beam illuminates a sample, light from a donut-shaped depletion laser beam is superimposed on the sample to suppress all its fluorescence except that from a nano-meter size point spread function in its centre. Moreover, conjugate donor-acceptor fluorescent probes have been used in the microscope to allow for switchable fluorescence at selectable wavelengths [6]. While research into the

selection of these probes has improved the resolution of the microscope, we propose a new technique for doing such.

The geometry of the point spread function of the STED microscope is established by the microscope's physical engineering. This implies that the resolution of the microscope is directly proportional to the visible light emitted from the focal plane. Therefore, being able to precisely control the visible fluorescence emitted by probes in the microscope would offer an optimization technique for improving its resolution.

Control engineering has been applied to photonic systems numerous times [7-10]. However, much of the previous work has required an accurate model of the system dynamics in order to provide effective control. Recently, photonic control has begun to focus on data-driven efforts in order to overcome model uncertainties and inaccuracies [11]. In this paper we seek to control the system for which the model is accurate up to a certain degree; i.e., the model uncertainties are bounded. Our control law, which does not require the exact model of the system, is constructed via tools from Model-Free Control and Sliding Control theory. The proposed controller is validated in numerical simulation against a *general* model of conjugate donor-acceptor fluorescent probes from Förster resonance energy transfer (FRET) theory [12-13]. This demonstrates the controller's robustness and flexibility to transfer to different microscope set-ups with different fluorescent probes. By precisely controlling probe fluorescence via automatic adjustment of the depletion laser beam pump power, the proposed controller improves the capabilities of the STED microscope.

METHODS

Modelling fluorescent probes using Förster resonance energy transfer

FRET describes the energy transfer relationship between conjugate donor-acceptor fluorescent probes. Donor molecules are excited by the excitation beam of the STED microscope. They then transfer their energy through FRET to their conjugate acceptor molecules. The wavelength of the STED laser beam is selected to be at the red end of the emission spectrum of the excited acceptors in order to cause rapid depletion of their excited state and supress the visible fluorescence emitted from the focal plane to improve the resolution of the microscope. A set of linear differential equations, Equation (1), reported in [6] describes the interactions between conjugate probes:

$$\begin{aligned}
\dot{x}_{da} &= k_d x_{Da} + (k_a + k_{STED}) x_{dA} - k_{exc} x_{da} \\
\dot{x}_{Da} &= k_{exc} x_{da} + (k_a + k_{STED}) x_{DA} - (k_d + k_F) x_{Da} \\
\dot{x}_{DA} &= k_{exc} x_{dA} - (k_a + k_{STED} + k_d) x_{DA} \\
\dot{x}_{dA} &= k_d x_{DA} + k_F x_{Da} - (k_a + k_{STED} + k_{exc}) x_{dA}
\end{aligned} \tag{1}$$

Here, capital and lowercase letters represent the excited and ground states, respectively. x_{ij} represents the population probability of the corresponding states, k_a and k_d represent the acceptor and donor fluorescent rates, k_{exc} represents the excitation rate of the donor, k_{STED} represents the STED rate of the acceptor, and k_F represents the FRET rate. Note that probe fluorescence described here behaves nonlinearly as excitation and STED rates increase, which is pivotal to super-resolution imaging. Acceptor fluorescence is given by:

$$F_a = k_a (x_{DA} + x_{dA}). \tag{2}$$

Data-driven Sliding Mode Control

Model-Free Control

In control engineering, given a dynamical system, feedback control is used to tailor the behaviour of the system in a desired manner. A dynamical system is any system with moving parts or variables that change with respect to an independent variable such as time. A laser system is a dynamical system. Typically, there are a set of time varying quantities associated with a system's behaviour that need to be controlled. If these quantities can be measured or observed externally, they are referred to as the outputs of the system, while the ones that cannot be measured or observed through external observation are referred to as the internal states of the system. The inputs of the system are a set of external signals that drive the system. Control strategies can be categorized into two fundamental groups: state-feedback, where the system outputs are controlled by adjusting the inputs based on the current state information, and output-feedback, where the adjustment of the inputs is done based on the current output. In the state-feedback regime, it is essential to have a mathematical representation of the dynamical system in the form of a system of differential equations, often known as the state-space realization of the system since the notion of state stems from the solutions of these differential equations. Therefore, state-feedback is inherently model-based. The output-feedback strategy can be further categorized into model-based output feedback and model-free output feedback. At the heart of the model-free output feedback control strategy is observing the outputs externally and feeding that information back to the controller which adjusts the inputs to achieve desired outputs without requiring any knowledge of the system model.

In the early 2010s, a robust model-free control method was developed by Fliess and Join [14], where the dynamics of the system are roughly estimated as follows

$$y^{(m)} = F(t) + \alpha u(t), \tag{3}$$

where y is the output of the system, $y^{(m)}$ is the m^{th} time derivative of the output, F accounts for the unknown dynamics and external disturbances of the system, α is an unknown parameter to be tuned and $u(t)$ is the input to the system. This is called the phenomenological model of the system. In systems with multiple inputs and multiple outputs (MIMO), y, F and u are vectors with multiple components. This set up will work for both MIMO and single-input-single-output (SISO) systems as long as the number of inputs is the same as the number of outputs. The goal here is to get the system output to track a desired output signal denoted by y_d, which is equivalent to diminishing the error signal defined as

$$e = y - y_d. \tag{4}$$

First, consider the dynamics of the error system having the following structure,

$$\sum_{i=n}^{m} K_i e^{(i)} = 0 \tag{5}$$

Here, $e^{(i)}$ denotes the i^{th} derivative of the error when i > 0, and the i^{th} iterative integral of the error when i < 0, while K_i denotes the constant coefficients to be determined. Since the error system takes the form of an ordinary linear differentio-integral equation with constant coefficients, it is well known that a set of $K_i, n \leq i \leq m$, exists such that the error system is exponentially stable. Exponential stability of the error system guarantees that the

error, e, will decay to zero at an exponential rate during a finite time. Now observe that from Equation (4), Equation (5) we have

$$y^{(m)} = y_d^{(m)} - \frac{1}{K_m}\left(\sum_{i=n}^{i=m-1} K_i\left(y^{(i)} - y_d^{(i)}\right)\right). \tag{6}$$

Then, the feedback control law can be derived from Equations (3) and (6) as follows:

$$u = \frac{1}{\alpha}\left(-F(t) + y_d^{(m)} - \frac{1}{K_m}\left(\sum_{i=n}^{i=m-1} K_i\left(y^{(i)} - y_d^{(i)}\right)\right)\right). \tag{7}$$

However, since $F(t)$ is unknown it is necessary to perform its approximation in real time. Since $F(t)$ is an integrable function, it can be approximated by piecewise constant functions on a small interval, T, and the approximation denoted by $\hat{F}$ can be computed as follows using the input u from the previous time step:

$$\hat{F} = \frac{1}{T}\int_{t-T}^{t}\left(y_d^{(m)} - \frac{1}{K_m}\left(\sum_{i=n}^{i=m-1} K_i\left(y^{(i)} - y_d^{(i)}\right)\right) - \alpha u\right) d\tau. \tag{8}$$

Notice that the feedback control law in Equation (7) does not require the knowledge of the model to achieve the control objective. Moreover, in the case where $m = 1$, the feedback law does not require the derivatives of the output; therefore, the controller stays robust even in the presence of noise at the output. The method is extremely powerful in cases where there are no reliable mathematical models available for the systems that need to be controlled. For our problem of FRET control, we consider a situation where a mathematical representation with limited reliability exists. Therefore, to leverage the available partial knowledge of the model, we also draw from Sliding Control, another control method, which is suitable for controlling systems with bounded uncertainties. Specifically, we use Fliess's phenomenological model in Equation (3) to approximate the dynamics of the system, which serves as our mathematical representation of the laser system dynamics with bounded uncertainties.

Sliding Control

Sliding Control is a well-developed theory from so-called "robust" control—a branch of control theory that focuses on systems with model uncertainties. This technique was developed in part by Slotine & Li in the early 1990s [15]. Here, we propose using the uncertain phenomenological model of the system dynamics from Model-Free Control in traditional Sliding Control. Doing so creates a model-free, exponentially stable controller.

Assume that the uncertain model of a system's dynamics is represented by Equation (3). Define a vector of measurable output error

$$\bar{e} = [e^{(n)}, \ldots, e^{(m)}]^T. \tag{9}$$

Here, the variable of interest is $e^{(n)}$, n may be any integer corresponding to the nth iterative derivative or integral, m is the order of Equation (3), and $m > n$. It is common practice to select $n = 0$ or -1 since these errors tend to be measurable in real time. Now, define a function

$$s(y,t) = \left(\frac{d}{dt} + \lambda\right)^{m-n-1} e^{(n)}. \tag{10}$$

Here $s = 0$ is termed *the sliding surface*, where $\lambda > 0$ and represents the *slope* of the sliding surface, which is chosen by the designer. The exponent $m - n - 1$ is chosen to be one less than the length of the error vector. The purpose of this equation is to replace a high order tracking problem with a 1st order stabilization problem. The goal of the controller will be to keep s equal to zero, which would result in all zero entries in $\bar{e}$. This is the same goal as Model-Free Control, which may lead one to notice the similarities between Equation (5) and Equation (10). For purposes that will be clear later, Equation (10) is rewritten as a binomial series in Equation (11).

$$s(y,t) = \sum_{k=0}^{m-n-1} \binom{m-n-1}{k} e^{(m-1-k)} \lambda^k \tag{11}$$

To ensure exponentially stable error dynamics, a control law must be chosen to satisfy

$$\frac{1}{2}\frac{d}{dt}s^2 \leq -\eta|s|\,, \tag{12}$$

which is called the "sliding condition". Here, η is a strictly positive real number. This inequality requires that the squared distance to the sliding surface strictly decreases, which makes the surface an invariant set. In other words, the output trajectories are guaranteed to reach the surface in finite time regardless of where they start. Given the sliding condition, the system's output trajectories "slide" along the sliding surface once they reach it—at which time it is in the "sliding mode":

$$\dot{s} = 0 \; = \sum_{k=0}^{m-n-1} \binom{m-n-1}{k} e^{(m-k)} \lambda^k. \tag{13}$$

From Equations (3) and (13), the approximated control effort at the current controller update can be defined as:

$$\hat{u} = \frac{1}{\alpha}\left(-\hat{F} + y_d^{(m)} - \sum_{k=1}^{m-n-1} \binom{m-n-1}{k} e^{(m-k)} \lambda^k\right). \tag{14}$$

Here, $\hat{F}$ represents the controller's approximation of the system dynamics using the control effort at the previous time step using numerical integration as is done in Model-Free Control. Note that $y^{(m)}$ does not need to be measured. Since this is only an approximation, the equivalent control (the control signal that ensures $\dot{s} = 0$) is said to be

$$u = \hat{u} - (k/\alpha) \cdot \mathrm{sgn}(s) \tag{15}$$

where $\mathrm{sgn}(s)$ is a discontinuous signum function such that

$$\mathrm{sgn}(s) = \begin{cases} +1 & if\ s > 0 \\ -1 & if\ s < 0\,' \end{cases} \tag{16}$$

and

$$k = \left|F - \hat{F}\right| + \eta \tag{17}$$

is chosen to satisfy Equation (12). The addition of the discontinuous term forces the output trajectory of the system closer to the desired given its current position relative to the sliding surface. While $\left|F - \hat{F}\right|$ is unknown, it is assumed to be bounded for well-behaved systems. Thus, choosing k sufficiently large will satisfy the sliding condition.

Traditional Sliding Mode Control focuses on driving state trajectories onto a desired path. Here, this technique was translated to the output-feedback problem to create a modern data-driven control strategy: Data-driven Sliding Control. For the purposes of this paper, $m = 1$ and $n = -1$ were chosen, which leads to the control law shown in Equation (18):

$$u = \frac{1}{\alpha}\left(-\hat{F} + \dot{y}_d - \lambda e\right) - \frac{k}{\alpha} \cdot \mathrm{sgn}(s). \tag{18}$$

A graphical representation of the implemented control scheme is shown in Figure 1. These parameters are chosen such that the derivative of the output, y, need not be measured as this is often difficult to do and laden with noise. The laser system depicted here can be replaced with most well-behaved systems and the controller will still work for a reasonable reference input because it does not require a model of the system in which it controls.

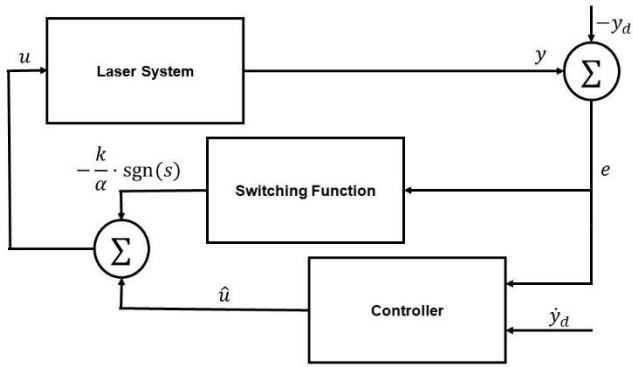

Figure 1: Data-driven Sliding Control Scheme when $m = 1, n = -1$.

NUMERICAL SIMULATION

The proposed Data-driven Sliding Controller was tested against a general model for FRET, Equation (1), in numerical simulation. While recent research has validated the FRET model [13], the controller described in this paper is inherently data-driven and model-free. Thus, uncertainties in this model do not affect the accuracy or validation of this controller. This is because the Data-driven Sliding Controller creates its own instantaneous model of the system at each controller update. The goal of the STED microscope is to limit the diffraction of light in the image plane to better resolve its subject. Thus, precisely controlled fluorescence emitted by the probes used in STED imaging is critical.

For simulation, the use of common, commercially available probes was assumed. Particularly, the FRET pair Cy3-Cy5, which have lifetimes of 0.3ns and 1ns, respectively. This gives the fluorescence rates $k_d = 1/0.3\ \text{ns}^{-1}$ and $k_a = 1\ \text{ns}^{-1}$. The FRET rate is directly related to the fluorescence rate of the donor and the efficiency of FRET: $k_F = k_d/(1/E - 1)$ where E represents the FRET efficiency. A moderate efficiency of 85% was assumed. The excitation laser was held at a constant power, which produced $k_{exc} = 20\ ns^{-1}$, and the STED laser pump power was automatically adjusted by the controller to vary k_{STED}. Moreover, the controller implemented in this simulation added a time varying "boundary layer" to the sliding surface to eliminate possible control "chattering" as done in [15]. This boundary layer eliminates excessive control activity when close to the sliding surface. The controller with boundary layer will track within a known precision—i.e. the width of the boundary layer. The low tracking error of the implemented controller verifies its precision.

Figure 2 (a) shows precisely controlled pulses of fluorescence from the acceptor probe achieved via automatic adjustment of the STED laser beam pump power by the Data-driven Sliding Controller. Figure 2 (b) shows the controlled STED rate achieved via automatic adjustment of the STED laser beam pump power. The controller demonstrated robust control with average error of 0.14% and peak error of 0.24%. This was achieved with control parameters: $\alpha = -1,\ \lambda = 25000, k = 1$. Since Equation (2) is made of population probabilities, normalized fluorescence is represented.

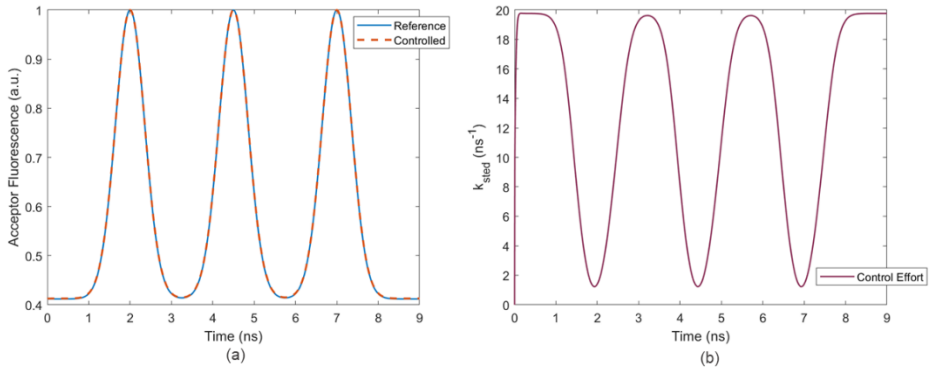

Figure 2: (a) Controlled pulses of acceptor fluorescence produced by the Data-driven Sliding Controller achieved via control parameters $\alpha = -1,\ \lambda = 25000,\ and\ k = 1$. (b) STED rate produced by the controller via automatic adjustment of the STED laser pump power.

Next, the effect of varying control parameters was explored. If the slope of the sliding surface is decreased to $\lambda = 2500$, high tracking performance is still achieved with an average error of 1.39% and peak error of 2.31%. Finally, reducing the slope another order of magnitude to $\lambda = 250$ produces an average error of 11.4% and peak error of 18.6%. Thus, increasing the slope increases the rate of convergence of the system output to the reference trajectory. This is shown in Figure 3. Then, to demonstrate the power of the data-driven controller, FRET parameters from the first simulation were changed arbitrarily to (1) $k_{exc} = 10\ \text{ns}^{-1}$, $E = 0.9$ and (2) $k_{exc} = 7\ ns^{-1}, E = 0.95,$ and $k_d = 1/0.5\ ns^{-1}$. All other FRET and control parameters were held constant. The output of the system still tracks the desired trajectory despite completely different system dynamics in both scenarios (1) and (2) without any controller adjustment. This is shown in Figure 4. In most experimental set ups, the measurable error of the system can be inherently noisy. To verify controller performance in this scenario, simulations were conducted with

Gaussian noise injected into the error signal. A single pulse is used in order to better observe the effects of the noise on the output signal. The results are shown in Figure 5 for varying levels of noise. A reasonable tracking performance is obtained for noise level below 5.8%.

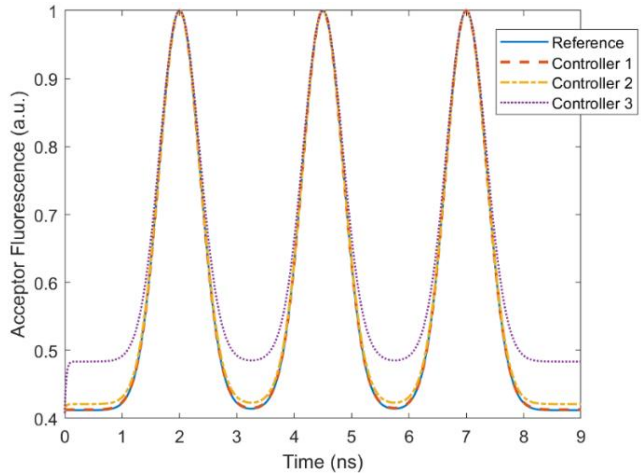

Figure 3: Degrading control with varying control parameters. Controller 1 corresponds to $\lambda = 25000$, controller 2 corresponds to $\lambda = 2500$, and controller 3 corresponds to $\lambda = 250$.

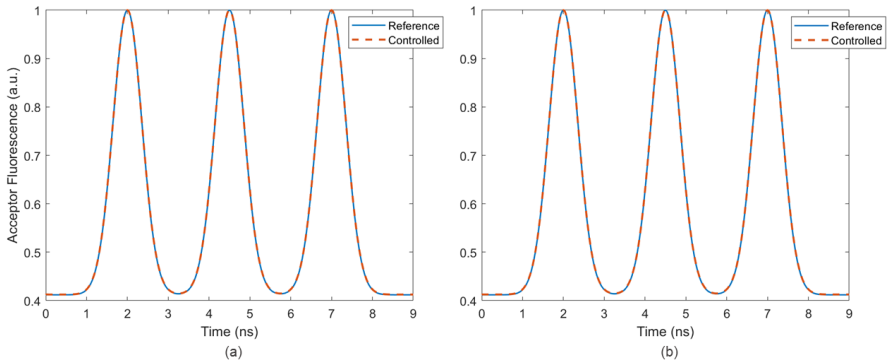

Figure 4: Controlled pulses of acceptor fluorescence after changing system dynamics. (a) Scenario 1: $k_{exc} = 10\ \mathrm{ns}^{-1}$ and $E = 0.9$. (b) Scenario 2: $k_{exc} = 7\ ns^{-1}, E = 0.95,$ and $k_d = 1/0.5\ ns^{-1}$.

CONCLUSIONS

A data-driven control method, Data-driven Sliding Control, was presented as a method for controlling the fluorescence from conjugate donor-acceptor probes in STED microscopy. The controller showed negligible tracking error in the presence of varying system dynamics and in the presence of Gaussian noise in its error signal without requiring control parameter adjustments. Since the geometry of its point spread function is established by the engineering of the microscope, its resolution is directly proportional to

the light emitted from the focal plane. By demonstrating how to precisely control the visible fluorescence emitted from probes in the focal plane of the microscope, this paper offers an optimization technique to increase the resolution of the STED microscope. In this paper, the microscope's excitation beam's pump power was held constant while the depletion laser beam was varied automatically by the controller. In the future, the authors plan to develop ways to automatically control both laser beams simultaneously, which would allow for the optimization of microscopes with dual-pulsed lasers and multiple probes' fluorescence.

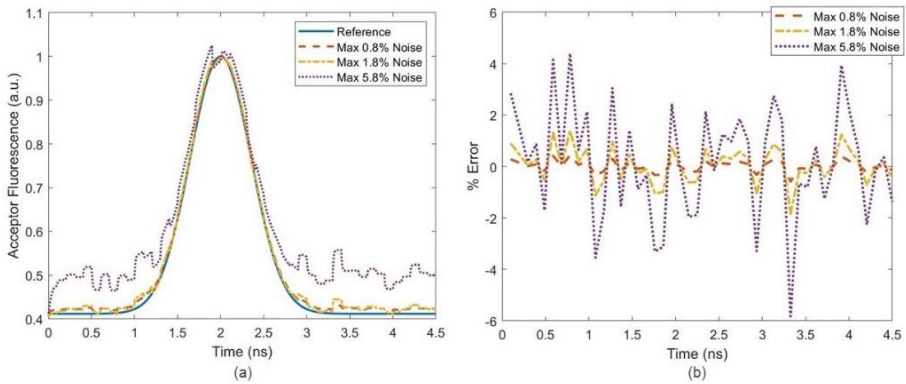

Figure 5: (a) Controlled pulses of fluorescence while gaussian noise was injected into the error signal of the controller. (b) The noise injected into the error signal over the course of the simulation measured in percent error. Percent error is calculated as the noise divided by the reference signal.

REFERENCES

[1] E. Abbe, *Archiv für Mikroskopische Anatomie* **9** (1), 413-468 (1873).
[2] P. Hanninen, L. Lehtela, and S. Hell, *Opt. Comm.* **130**, 29-33 (1996).
[3] T. Klar, E. Engel, and S. Hell, *Phys. Rev. E.* **64**, (2001).
[4] Y. Liu, Y. Lu, X. Yang, X. Zheng, S. Wen, F. Wang, X. Vidal, J. Zhao, D. Liu, Z. Zhou, C. Ma, J. Zhou, J. Piper, P. Xi, and D. Jin, *Nature* **543**, 229-233 (2017).
[5] G. Paes, A. Habrant, C. Terryn, *Plants* **7** (1), 11-21 (2018).
[6] S. Deng, J. Chen, Z. Gao, C. Fan, Q. Yan and Y. Wang, *J. Micro.* **269** (1), 59-65 (2018).
[7] M. Thitsa and T. Q. Ta in Mathematical and Computational Aspects of Materials Science, (Mater. Res. Soc. Symp. Proc. **1753**, Boston, MA, 2014) pp. 08-18.
[8] M. Thitsa, Z. Rice, M. Nve-Nsi, and X. Xue, ECS Transactions **75** (11), 59-66 (2016).
[9] S. Williams, M. Thitsa, and X. Xue, ECS Transactions **69** (12), 61-69 (2015).
[10] R. Cai, M. Thitsa, A. Bluiett, E. Brown, and U. Hommerich, *Opt. Mat.*, **68**, 19-23 (2017).
[11] B. Simon, J. Dupaty, E. Brown, and M. Thitsa, *MRS Adv.* **4** (11-12), 683-688 (2019).
[12] T. Förster, *Die Naturwissenschaften* **33** (6), 166-175 (1946).
[13] C. Cortes and Z. Jacob, *Opt. Exp.* **26** (15), 19371-19387 (2018).
[14] M. Fliess and C. Join, *Int. J. Control* **86**, 2228- 2252 (2013).
[15] J. Slotine and W. Li, *Applied Nonlinear Control*, (Prentice Hall, Englewood Cliffs, 1991), pp. 276-310.